High-resolution CT-derived measures of lung density are valid indexes of interstitial lung disease

PATRICK G. HARTLEY, JEFFREY R. GALVIN, GARY W. HUNNINGHAKE, JAMES A. MERCHANT, STEPHEN J. YAGLA, STEPHEN B. SPEAKMAN, AND DAVID A. SCHWARTZ

Pulmonary Disease Division, Departments of Internal Medicine, Radiology, and Preventive Medicine, and Veterans Administration, The University of Iowa, Iowa City, Iowa 52242

Hartley, Patrick G., Jeffrey R. Galvin, Gary W. Hunninghake, James A. Merchant, Stephen J. Yagla, Stephen B. Speakman, and David A. Schwartz. High-resolution CT-derived measures of lung density are valid indexes of interstitial lung disease. *J. Appl. Physiol.* 76(1): 271–277, 1994. —To assess the validity of computer-assisted methods in analyzing the lung parenchyma imaged with high-resolution computed tomography (HRCT), we compared computer-derived estimates of lung density to other, more traditional, measures of parenchymal injury in 24 subjects with idiopathic pulmonary fibrosis (IPF) and 60 subjects with extensive occupational exposure to asbestos. Gray scale density histograms were constructed from the HRCT images. The gray scale histogram of both study groups was of a skewed unimodal distribution. However, compared with the asbestos-exposed subjects, the patients with IPF had a gray scale distribution that was significantly shifted to the right (greater density) and flatter. In a multivariate analysis, after controlling for age and cigarette smoking, we found that the mean and median gray scale densities were independently associated with the presence of moderate-to-severe dyspnea, a higher International Labour Office chest X-ray category, a lower forced vital capacity, and a higher concentration of macrophages and eosinophils in the bronchoalveolar lavage fluid. These factors accounted for >70% of the variance of the mean and median gray scale densities. Interestingly, no differences in gray scale density measures were noted between patients with IPF and patients with asbestosis when these other factors were taken into account. Our results suggest that computer-derived density analysis of the lung parenchyma on the HRCT scan is a valid, clinically meaningful, and objective measure of interstitial lung disease.

asbestosis; pulmonary fibrosis; computed tomography; X ray; image analysis

CHEST RADIOGRAPHS have become a cornerstone in diagnosing and assessing the extent and severity of interstitial lung disease. However, concerns exist regarding the sensitivity and specificity of this diagnostic technique. For instance, between 9.6 and 18.1% of individuals with pathological evidence of interstitial lung disease will have a normal chest radiograph (7, 10, 19). Moreover, the interpretation of standard chest radiographs using either descriptive terminology or the International Labour Office (ILO) classification system has proved problematic in terms of inter- and intrareader reliability. Specifically, interreader agreement ranges from 67 to 90% for ILO major profusion categories, and there is only 75% agreement on the quality of the chest X ray (25, 27). Similar rates of interreader agreement were reported for the interpretation of radiographs of patients with tuberculosis (37, 38). Importantly, intrareader agreement appears to yield similar results, with readers agreeing with their previous interpretation (in terms of stability, progression, or improvement) on only 78% of the films (38).

High-resolution computed tomography (HRCT) clearly improves the visual clarity of the lung parenchyma compared with the standard chest X ray (22). Unfortunately, there is little information to suggest that subjective HRCT interpretation is any more reliable than subjective chest X-ray interpretation (4). Importantly, an objective standardized system to grade the interstitial lesions on the HRCT scan has not been developed. Moreover, the pathological validity of the parenchymal abnormalities noted on HRCT has not been fully evaluated. Thus, further work needs to be pursued to identify an objective and reliable grading system for the clinical assessment of parenchymal abnormalities on the HRCT scan.

Computerized approaches to image analysis have been used to identify central nervous system pathology (26), plan orthopedic procedures (29) and maxillofacial surgery (8), and assess a number of features of cardiac function (13, 32). Computer-assisted analysis of chest radiographic images has been studied in the context of digitized screening chest X rays for coin lesions or pneumoconioses (17, 34) and density analysis of computed tomography (CT) images to quantify emphysema (12, 18, 23). We have used computer-derived quantitative methods to determine the relationship between asbestos-induced pleural fibrosis and restrictive lung function (31). Application of this technology in evaluating interstitial abnormalities in the lung parenchyma might address several problems inherent in the traditional subjective assessment of either the chest X ray or the HRCT scan. Moreover, this measure of interstitial lung disease would provide an objective and reproducible measure of the radiographic extent of interstitial lung disease that would not be subject to observer bias.

In this study, we tested the hypothesis that a computer-derived quantitative analysis of lung parenchymal density on the chest HRCT scan would be a valid measure of interstitial lung disease compared with standard clinical, radiological, physiological, and biological indexes of disease activity. In addition, we postulated that when we controlled for confounders, such as the severity of parenchymal abnormality on chest X ray, there would be no difference in gray scale density between patient populations with different types of interstitial lung disease. To address these hypotheses, we analyzed the lung density on HRCT images from 60 asbestos-exposed subjects and 24 subjects with idiopathic pulmonary fibrosis

TABLE 1. *Demographic and clinical characteristics of study population*

	IPF	Asbestos Exposed
n	24	60
Sex		
Male	15 (62.5%)	60 (100%)
Female	9 (37.5%)	0 (0%)
Age, yr	63.4±12.5	61.9±8.8
Smoking history		
Never	8 (33.3%)	13 (21.7%)
Former	14 (58.3%)	39 (65%)
Current	2 (8.3%)	8 (13.3%)
Pack-years	24.38±21.79	28.22±23.03
Chest X ray		
ILO category		
0	1 (4.2%)	41 (68.3%)
1	10 (41.7%)	18 (30%)
2	11 (45.8%)	1 (1.7%)
3	2 (8.3%)	0
Pleural disease		
Present	5 (20.8%)	39 (65%)
Absent	19 (79.2%)	21 (35%)
Dyspnea class		
1	2 (8.3%)	29 (48.3%)
2	8 (33.3%)	21 (35%)
3	1 (4.2%)	3 (5%)
4	6 (25%)	4 (6.7%)
5	7 (29.2%)	3 (5%)

Values are means ± SD for age and pack-years; *n*, no. of subjects. IPF, idiopathic pulmonary fibrosis; ILO, International Labour Office.

(IPF) and then investigated the relationship between these measures of lung density and other test results to validate this measure of interstitial lung disease in these populations.

METHODS

Study population. The subjects for this investigation were identified as part of our ongoing Specialized Center of Research Program in interstitial and occupational lung disease. Our study population consisted of 60 asbestos-exposed subjects and 24 subjects with IPF. The demographic characteristics are outlined in Table 1. The asbestos-exposed subjects were identified primarily through the Sheet Metal Worker's 1986 Screening Program (30). In addition, several asbestos-exposed subjects were enrolled through the Occupational Medicine Clinic at the University of Iowa. All asbestos-exposed subjects had at least 1 yr of occupational exposure in a high-exposure setting (i.e., direct contact with asbestos), and a minimum of 20 yr was required between first exposure to asbestos and entry into the study. Subjects with asbestos-induced parenchymal fibrosis (i.e., asbestosis) and asbestos-induced pleural disease were preferentially included in this study. However, asbestos-exposed subjects without obvious lung disease were also included. In the subjects with IPF, the diagnosis was made on the basis of a consistent clinical history, interstitial fibrosis on chest X ray, and pulmonary function tests demonstrating either restrictive lung function or abnormal gas exchange. Importantly, all patients with IPF were required not to have a clinical history of collagen vascular disease or of exposure to environmental agents known to cause interstitial lung disease. An open lung biopsy was obtained in 19 of the 24 subjects with IPF, and a consistent histological picture was obtained on transbronchial biopsy in two other cases. All biopsies were cultured for mycobacteria and fungi. The diagnosis in the remaining three cases was made on clinical criteria, as histological confirmation was not available.

Pulmonary function testing. The pulmonary function tests consisted of standard spirometry using a Medical Graphics 1070 system (St. Paul, MN) and lung volumes via the body plethysmography Medical Graphics 1085 system. Single-breath pulmonary diffusing capacity of CO (DL_{CO}) was measured using the Medical Graphics 1070 system. The measurements of lung function were performed using standard protocols, and the American Thoracic Society guidelines (5) were used to determine acceptability. The predicted normal values were those of Morris et al. (21) for spirometry, Goldman and Becklake (11) for lung volumes, and Van Ganse et al. (35) for DL_{CO}.

Dyspnea assessment. The dyspnea level was assessed by questionnaire (9) administered by one observer who was blinded to the clinical data. This classification system comprises five grades of dyspnea. Class 1 dyspnea is breathlessness that is consistent with the circumstances of the activity. Class 2 dyspnea is characterized by breathlessness when hurrying on the level or walking up a slight hill. Class 3 dyspnea is characterized by an inability to keep pace with others of the same age on the level because of breathlessness. Class 4 dyspnea occurs during such activities as climbing a flight of stairs or walking 100 yd (or after a few minutes) on the level at one's own pace. Class 5 dyspnea may prevent the subject from leaving the house or may occur while performing activities of daily living such as dressing.

Chest radiographs. Chest radiographs were performed in the posteroanterior projection on all study subjects and were individually interpreted by three experienced readers who used the ILO 1980 classification of radiographs of pneumoconioses (14). Each reader was blinded to the exposure history, the clinical data, and the opinions of the other readers when interpreting the radiographs. Agreement between at least two of the three readers was required to identify the ILO major category of perfusion. In the unusual case where all three readers identified a different major ILO category (1 IPF patient and none of the asbestos-exposed subjects), the median reading was chosen. In the asbestos-exposed subjects, we defined asbestosis as an ILO major category of ≥ 1.

Bronchoalveolar lavage (BAL). Fiber-optic bronchoscopy and BAL were performed on 58 asbestos-exposed subjects and 21 subjects with IPF with use of our standard technique (39). Subjects were premedicated with atropine and meperidine hydrochloride. The upper airway was anesthetized with aerosolized 4% lidocaine. The bronchoscope was advanced into the airways, and the tip was maintained in the wedged position in a subsegmental bronchus throughout the lavage procedure. In all cases, two lavages were performed, usually in subsegments of the right middle lobe and lingula. Each lavage consisted of 120 ml of saline (6 × 20-ml aliquots), and the fluid retrieved from the first aliquot was discarded. The remaining lavage fluid was filtered through two layers of gauze and centrifuged at 1,500 rpm for 5 min. The cell pellet was washed twice in Hanks' balanced salt solution without Ca^{2+} or Mg^{2+}. Cell counts and differentials were determined with a hemocytometer (Coulter Electronics, Hialeah, FL). The cells were washed once more and resuspended in RPMI 1640 medium so that the final concentration was 10^7 cells/ml. The cells present in 10–12 μl of the 10^7-cells/ml cell suspension were spun onto a glass slide with the use of a filter card and a cytocentrifuge (Cytospin2, Shanden Southern, Sewickley, PA). After the cells were dried for 2 min, they were stained using a Diff Quik Stain set (Harleco, Gibbstown, NJ). The cells were counted and classified only after the cytocentrifuge preparation was thought to be satisfactory by the following criteria: negligible staining artifact, uniform dispersal of cells without clumping, essentially no disruption of cells, and <3% airway epithelial cells. The results from both lavaged lung segments were averaged, and, unless other-

wise stated, cell counts are expressed as 10^4 cells per milliliter of BAL fluid return.

Chest HRCT. HRCT scans of the lung were obtained on all study subjects by using an Imatron C-100 ultrafast scanner. Images were obtained at full inspiration with the subject prone. A high spatial frequency algorithm was used to reconstruct the image data, and the smallest possible scanning circle was employed to maximize the resolution. The scanning time was 0.6 s. Three-millimeter images were obtained every 2 cm from the apex of the lungs to the diaphragms.

Computer-derived density measurements. The steps involved in the construction of a radiographic image of the lung included *1*) identification of tomographic images that encompass the entire lung, *2*) identification of the spatial position and orientation of each tomographic image, *3*) identification of the actual region of interest (lung, pleura, mediastinum, etc.), *4*) reconstruction and display of the two-dimensional image, and *5*) extraction of quantitative data. Data generated from the HRCT scan were directly transferred to a Silicon Graphics 4D Iris Workstation (Mountain View, CA) and were digitized in a 512 × 512-pixel matrix with 16-bit gray level resolution. The lung parenchyma for each lung image was traced and defined as individual regions of interest. To correct the gray scale density measures for variations in CT scanning techniques, we standardized each measure of density to the frequency distribution of tracheal air (−1,000 Hounsfield units) and column of blood in the aorta (0.0 Hounsfield units) on each HRCT scan. A specifically designed program plotted a frequency histogram of pixels for each gray scale value within this reference range for each lung. Gray scale frequency histograms for each lung and for the combined lung parenchyma of each subject were plotted. The mean, median, kurtosis (peakedness), and skewness of the gray scale frequency histogram for each subject were calculated using standard statistical techniques.

Statistics. Because the primary interest of the study was to assess the validity of computer-derived indexes as measures of the extent and activity of interstitial lung disease, we compared the mean, median, kurtosis, and skewness of the gray scale frequency histograms between both subject groups (IPF vs. asbestos exposed) and among ILO chest X ray categories by using univariate statistics (6). Although kurtosis and skewness are seldom used in statistical analyses, these measures are very helpful in statistically describing a histogram. The gray scale density measures were compared with the subjects' age, pack-years of cigarette smoking, BAL cellularity, and pulmonary function tests by using correlation coefficients. Parametric and nonparametric approaches to the univariate analysis were used appropriately (6).

Multivariate linear regression modeling was used to test the independent determinants of mean and median gray scale densities after controlling for the effect of possible confounders such as age and smoking history (20). The regression models were developed by individually assessing the relationship between gray scale density (mean and median) and each of our independent measures of interstitial lung disease while controlling for potential confounders. Multivariate models were further developed by simultaneously entering multiple measures of interstitial lung disease to assess the independence of their contribution. The overall aim of these multivariate models was to determine the validity of gray scale measures of density after controlling for potential confounders and also to evaluate whether the gray scale measure of lung density served as a comprehensive measure for interstitial lung disease.

RESULTS

Our study population consisted of 24 patients with IPF and 60 subjects who had been exposed to asbestos. Demographic, clinical, radiological, and pulmonary function data on our study subjects are given in Tables 1 and 2. All of our asbestos-exposed subjects were males with significant occupational exposure, whereas males accounted for 62.5% of our patients with IPF. Over 60% of subjects in both study groups were either former or current cigarette smokers. There was no significant difference in mean pack-years of cigarette smoking between the IPF group and the asbestos-exposed group. Nine of the IPF patients were taking oral prednisone, and one patient was taking prednisone and cyclophosphamide at the time of the study. None of the asbestos-exposed subjects was taking immunomodulating agents. Our asbestos-exposed group included a large number of subjects (68.3%) whose lung parenchyma appeared radiologically normal by ILO criteria (category 0) compared with only one subject in our IPF study group. The larger proportion of subjects with radiologically apparent parenchymal disease in the IPF group is reflected in the difference between subjective complaints of dyspnea, with 59% of IPF patients compared with 17% of the asbestos-exposed subjects reporting moderate-to-severe dyspnea (dyspnea class 3–5). In addition, significant differences in the percent predicted total lung capacity, residual volume, forced vital capacity (FVC), and D_{LCO} were noted during pulmonary function testing between both study groups. Limiting the analysis to subjects with ILO category 1 chest X rays (the only ILO category with reasonable numbers in both study groups), patients with IPF still had significantly worse lung function than patients with asbestosis. In fact, even within this radiographic subgroup, 70% of IPF patients complained of moderate-to-severe dyspnea compared with only 17% of patients with asbestosis.

TABLE 2. *Pulmonary function in patients with IPF compared with asbestos-exposed subjects*

	IPF	Asbestos Exposed
n	24	60
TLC	79.5±20.2	109.9±16.7*
RV	80.2±23.5	122.2±38.5*
FVC	72.5±21.3	88.6±14.5*
FEV_1	80.2±20.0	89.1±19.7
D_{LCO}	52.8±19.4	105.2±18.2*
FEV_1/FVC	70.5±3.9	71.2±9.9

Values are means ± SD as %predicted except ratio of forced expiratory volume in 1 s (FEV_1) to forced vital capacity (FVC); *n*, no. of subjects. TLC, total lung capacity; RV, residual volume; D_{LCO}, diffusion capacity for CO. * $P < 0.05$ vs. IPF.

On visual and statistical inspection of the computer-derived gray scale histograms, it was noted that the histograms of all study subjects were of a unimodal distribution with a skewed long tail to the right, toward increasing gray scale density. The subjects with IPF, however, had a distribution that was more shifted to the right and flatter (lower kurtosis) than that of the asbestos-exposed group (Table 3). All measured parameters (mean, median, kurtosis, and skewness) of the gray scale distribution were significantly different between patients with IPF and subjects who had been exposed to asbestos, reflecting the more advanced changes in chest radiographs noted in our IPF patients. When we limited the analysis to study subjects with category 1 radiographs, patients

TABLE 3. *Comparison of gray scale density derived from HRCT scans between patients with IPF and asbestos-exposed subjects*

	IPF	Asbestos Exposed	*P*
n	24	60	
Mean	−749.1±53.9	−825.2±32.2	<0.001
Median	−811.6±53.7	−877.7±28.0	<0.001
Kurtosis	2.56±2.01	7.63±2.35	<0.001
Skewness	1.57±0.46	2.63±0.37	<0.001

Values are means ± SD in Hounsfield units; *n*, no. of subjects. HRCT, high-resolution computed tomography.

with IPF still had significant increases in the mean and median gray scale densities compared with those with asbestosis (data not shown). However, there was no significant difference for kurtosis and skewness between study groups within this radiological category.

The gray scale density was found to be significantly related to several other measures of interstitial lung disease. When the total study population was analyzed, a significant difference in gray scale density measurement was noted between those with and without parenchymal lung disease in the chest radiograph (Table 4, Fig. 1). Obvious consistent trends in gray scale density were apparent, as the degree of interstitial lung disease increased on the standard chest X ray. In addition, significant correlations existed between measures of gray scale density and pulmonary function (total lung capacity, residual volume, FVC, forced expired volume in 1 s, and DL_{CO}), suggesting higher mean and median gray scale densities, and a flatter and broader distribution was associated with more restrictive lung function and diminished gas exchange as measured by DL_{CO} (Table 5). In addition, there was a significant relationship between higher concentration of cells (macrophages, neutrophils, and eosinophils) in the BAL fluid (expressed as 10^4 cells/ml of BAL fluid return) and higher mean and median gray scale densities on the frequency distribution histogram (Table 5). Interestingly, there was a significant negative correlation between the percentage of lymphocytes in the BAL fluid and the higher mean and median gray scale densities.

To further define the validity of the density measures in the context of other, more traditional, measures of interstitial lung disease, we used multivariate techniques (Table 6). In particular, we were interested in identifying the clinical features of interstitial lung disease that were independently related to the mean and median gray scale densities while controlling for the subjects' age and smoking history. After exploring several possible models, the most powerful solution with the least number of terms was a model that showed that higher mean and median gray scale densities were independently associated with the presence of moderate-to-severe dyspnea (i.e., class 3–5), a higher ILO category of interstitial lung disease on chest X ray, a lower FVC, and a higher concentration of macrophages and eosinophils in the BAL fluid (Table 6). In fact, these models accounted for >70% of the variance of the mean and median gray scale densities. Interestingly, the subjects' diagnosis (i.e., IPF or asbestosis) was not independently related to these measures of lung density when these other factors were taken into account. Alternative multivariate models that included the study group (IPF vs. asbestos exposed) explained less of the variance of the mean and median gray scale densities and eliminated the assigned ILO chest X-ray category from the model.

TABLE 4. *Relationship of HRCT-derived gray scale density to chest X-ray ILO category*

	ILO Category				
	0	1	2	3	*P*†
Mean	−832.9	−790.5*	−747.0*	−706.5*	<0.0001
Median	−883.7	−846.6*	−813.2*	−779.5*	<0.0001
Kurtosis	8.1	5.4*	2.3*	0.5*	<0.0001
Skewness	2.7	2.2*	1.5*	1.1*	<0.0001

Values are in Hounsfield Units. * $P < 0.05$ vs. ILO category 0. † Test for trend.

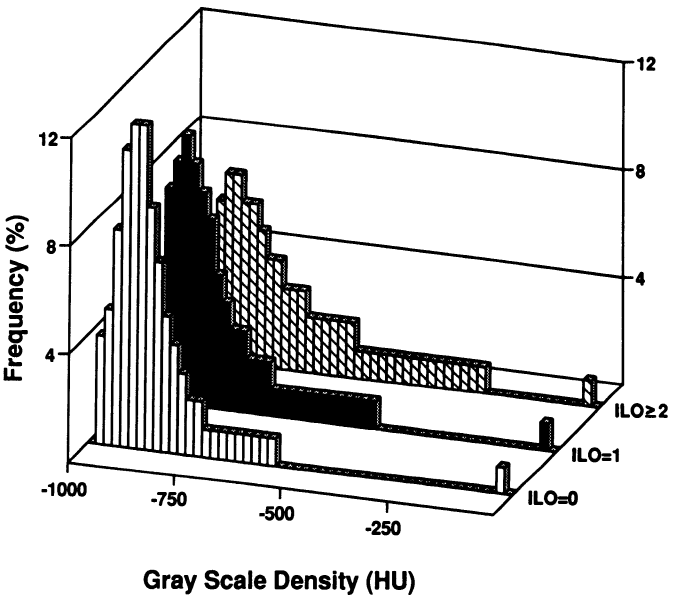

FIG. 1. Frequency histogram of gray scale density by chest X-ray International Labour Office (ILO) major category for all study subjects. HU, Hounsfield units.

TABLE 5. *Relationship between measures of gray scale density and both pulmonary function and BAL cellularity*

	Gray Scale Density			
	Mean	Median	Kurtosis	Skewness
Pulmonary function				
FEV_1	−0.43*	−0.39*	0.46*	0.50*
FVC	−0.61*	−0.58*	0.61*	0.64*
FEV_1/FVC	0.09	0.14	0.05	0.04
TLC	−0.67*	−0.65*	0.62*	0.67*
RV	−0.45*	−0.43*	0.39*	0.43*
DL_{CO}	−0.62*	−0.57*	0.70*	0.74*
BAL cellularity, $\times 10^4$ cells/ml BAL fluid				
Macrophages	0.36*	0.41*	−0.18	−0.19
Lymphocytes	−0.05	−0.03	0.07	0.06
Neutrophils	0.43*	0.43*	−0.44*	−0.46*
Eosinophils	0.39*	0.37*	−0.41*	−0.44*

Values given are correlation coefficients. Absolute values of pulmonary function variables were considered in analysis. BAL, bronchoalveolar lavage. * $P < 0.001$.

TABLE 6. *Multiple linear regression models that best identified determinants of mean and median gray scale densities*

	Mean Gray Scale Density		Median Gray Scale Density	
	β	P	β	P
Dyspnea class 3–5	21.0±8.1	0.01	19.7±7.5	0.01
ILO				
Category 1	20.7±7.8	0.01	15.4±7.2	0.04
Category 2–3	62.7±10.2	0.0001	50.3±9.4	0.0001
FVC	−19.0±4.1	0.0001	−17.7±10.8	0.0001
BAL eosinophils, ml^{-1}	0.261±0.090	0.005	0.287±0.083	0.001
BAL macrophages, ml^{-1}	0.050±0.019	0.01	0.041±0.018	0.025
Constant	−721.9±36.2	0.0001	−755.9±33.6	0.0001
Model R^2	0.72		0.71	
F	17.34 (10, 68)		16.69 (10, 68)	

β values (regression coefficients) are means ± SE; degrees of freedom for F values are in parentheses. Models were controlled for age, smoking status, and pack-years of cigarette smoking.

DISCUSSION

Our findings indicate that the assessment of parenchymal density on the HRCT scan is a valid measure of the extent of interstitial lung disease. This conclusion is supported by our observation of an independent relationship between computer-derived measures of lung density and symptoms of dyspnea, increasing interstitial lung disease on the chest X ray, restrictive physiology, and biological indexes of inflammation. Furthermore, our results suggest that measurements of lung density appear to be a composite measure of interstitial lung disease that is independently related to radiographic, physiological, and biological indexes of disease. Moreover, our results suggest that computer-derived estimates of lung density may prove to contain information regarding the extent and severity of interstitial lung disease that is not provided by traditional diagnostic tools that are currently used to evaluate patients with this disease. In the most limited context, our results indicate that computer-assisted measures of lung density objectively define the radiographic extent of interstitial lung disease.

The validity of the computer-derived measures of gray scale density is supported by the consistent relationship observed between measures of lung density and other indexes of interstitial lung disease such as dyspnea, ILO profusion, restrictive lung function, and BAL cellularity. Importantly, we found that moderate-to-severe dyspnea, higher ILO chest X-ray category, restrictive physiology, and higher concentrations of macrophages and eosinophils in the BAL fluid were all independently related to the computer-derived parenchymal density measures, explaining >70% of the variance of both the mean and median measures of density. However, after accounting for these factors, the gray scale density was unable to distinguish IPF from asbestos-related parenchymal abnormalities. In contrast, subjective interpretation of the HRCT scan may be able to distinguish these two types of interstitial lung disease by the presence of abnormalities such as subpleural curvilinear lines and parenchymal bands, both of which are thought to be characteristic but not pathognomonic of asbestosis (1, 22, 33). We have not examined the relationship of gray scale density to specific descriptive abnormalities on the HRCT scan or to histopathological findings in terms of specific pathological patterns of disease. Instead, we chose to validate our technique against more commonly used radiographic, physiological, and biological indexes of the activity and extent of interstitial lung disease. Our observations strongly suggest that objective interpretation of the HRCT scan provides a valid measure of the extent of interstitial lung disease.

The pathological significance of specific descriptive abnormalities on the HRCT scan such as ground glass infiltrate has not been adequately studied. However, the suggestion has been made that these radiographic abnormalities represent either filling of the air spaces with histiocytes and alveolar septal inflammation, suggesting disease activity (24), or thickening of alveolar walls by fibrosis or edema (3). Further work needs to be pursued to define the relationship of both the visual and computer-derived measures of the lung parenchyma on the HRCT scan to histopathological patterns of disease. In view of the heterogeneous distribution of parenchymal abnormalities on the HRCT scan, the gray scale density of specific segments of lung parenchyma should be compared with both BAL cellularity and basic lung histology. In our study, we applied gray scale density analysis to the entire lung parenchyma of study subjects rather than to specific regions of parenchymal infiltration. This approach yields an average gray scale density for each subject, which may underestimate or obscure the regional differences in disease distribution known to exist in interstitial lung disease. Other computer-derived measures of parenchymal abnormalities, such as analysis of texture, may provide more information on patterns of disease activity than is available from gray scale density. Texture analysis has already been used to evaluate digitized chest X rays in screening for pneumoconioses (17, 34). A similar technique may be applicable to the HRCT scan in interstitial lung disease. Because texture represents the spatial distribution of lung density, this may be particularly important in assessing disease heterogeneity in different types of interstitial lung disease.

One of the principal advantages of assessing lung density is its inherent objectivity. The subjective nature of chest X-ray interpretation and the lack of inter- and intrareader reliability in evaluating chest films from subjects at risk of interstitial lung disease have been well documented (25, 27). Objective approaches using computerized textural analysis of digitized chest X rays in screening for infiltrative lung diseases have been evaluated (17, 34) but as yet remain largely a research tool. Interpretation of the HRCT scan in interstitial lung disease has relied on descriptive terminology thought to correlate with known histological patterns observed in these processes. Al Jarad et al. (4) recently published a visual HRCT scoring system analogous to the ILO system, which they have evaluated in patients with asbestos-related pulmonary fibrosis, pleural disease, and emphysema. Interestingly, inter- and intraobserver agreement

was slightly improved (compared with the ILO system) using the visual scoring system that they developed for the HRCT scan. Inter- and intraobserver agreement for the presence of parenchymal fibrosis was, respectively, 96 and 99% for HRCT score compared with 90 and 95% for chest X ray interpretation. Importantly, a computerized approach to quantify the gray scale density on the HRCT scan will overcome potential problems with inter- and intrareader reliability and will also effectively address problems with observer bias.

It is interesting to speculate whether the information yielded by this quantitative approach to the HRCT scan in interstitial lung disease represents a potentially new diagnostic tool or merely duplicates information readily available from the indexes currently used to assess the extent and activity of the parenchymal fibrosis. Obviously, some of the information overlaps that provided by patient symptoms, the degree of interstitial lung disease on the chest X ray, the interpretation of pulmonary function tests, and the cellular analysis of BAL fluid. However, our results suggest that these computer-derived measures of lung density yield a more comprehensive index of interstitial lung disease than traditional methods of evaluation. Individually, the clinical assessment, chest roentgenograms, pulmonary function tests, and BAL cellularity are helpful in the evaluation of suspected interstitial lung disease but do not provide a comprehensive index of interstitial lung disease. In fact, clinicians rely on the combination of these results with histological information (except in cases of asbestosis) to make a diagnosis of interstitial lung disease or decide on a management strategy. Importantly, the combination of these more conventional methods of assessing interstitial lung disease explains 70% of the variance in the gray scale density measures. However, 30% of the gray scale density remains unexplained by traditional measures of lung disease, suggesting that the gray scale density may provide additional clinical information not available in the traditional diagnostic tools. Our results lead us to speculate that measures of lung density may provide a unique assessment of the interstitial process that will complement and enhance the traditional diagnostic tools that are used to assess interstitial lung disease.

Because the lung density on HRCT is a reflection of the relative distributions of air, tissue, blood, and extravascular fluid within the lung, it is important to standardize the degree of inspiration. It has been shown that considerable differences in gray scale density exist between measures taken at various phases of the respiratory cycle (15, 28, 36). Although some have suggested that this should be rigidly controlled by spirometric gating of the CT scanner (16), the majority of published studies using CT-derived lung density (2, 12, 18, 23), mainly in patients with emphysema, have simply asked patients to hold the breath at full inspiration. This is the method of HRCT scanning we chose to adopt in our study. Although it is claimed that the degree of inspiration during voluntary breath holding is not always reproducible (15), in a large series of HRCT scans, such as in our study, variability in the degree of inspiratory breath holding would be a random occurrence, tending to bias our results toward the null and strengthening any subsequently observed statistical differences.

In summary, we have used computer-assisted methods to analyze the gray scale density of the lung parenchyma of subjects with IPF and subjects occupationally exposed to asbestos. We have found that these measures of disease are valid in relation to other accepted methods of assessing interstitial lung disease. Moreover, these computer-derived measures of lung density appear to represent a comprehensive measure of interstitial lung disease that may yield information above and beyond that available in the diagnostic tools that are traditionally used to assess the extent and activity of pulmonary fibrosis.

The authors thank Boyd Knosp and the Image Analysis Facility at the University of Iowa for expertise and assistance in this project.

This study was supported by National Heart, Lung, and Blood Institute (NHLBI) Specialized Center of Research Grant HL-37121; National Institute of Occupational Safety and Health of the Centers for Disease Control Grant OH-00093-01; and the Asbestos Victims Special Fund Trust. P. G. Hartley is supported by NHLBI National Research Service Award Fellowship Training Grant HL-07638. D. A. Schwartz is a recipient of National Institute of Environmental Health Sciences Clinical Investigator Award ES-00203.

Address for reprint requests: P. G. Hartley, Pulmonary Disease Div., Dept. of Internal Medicine, Univ. of Iowa College of Medicine, Iowa City, IA 52242.

Received 24 June 1993; accepted in final form 26 August 1993.

REFERENCES

1. **Aberle, D. R., G. Gamsu, C. S. Ray, and I. M. Feuerstein.** Asbestos-related pleural and parenchymal fibrosis: detection with high-resolution CT. *Radiology* 166: 729–734, 1988.
2. **Adams, H., M. S. Bernard, and K. McConnochie.** An appraisal of CT pulmonary density mapping in normal subjects. *Clin. Radiol.* 43: 238–242, 1991.
3. **Akira, M., S. Yamamoto, K. Yokoyama, N. Kita, K. Morinaga, T. Higashihara, and T. Kozuka.** Asbestosis: high-resolution CT-pathologic correlation. *Radiology* 176: 389–394, 1990.
4. **Al Jarad, N., P. Wilkinson, M. C. Pearson, and R. M. Rudd.** A new high resolution computed tomography scoring system for pulmonary fibrosis, pleural disease and emphysema in patients with asbestos related disease. *Br. J. Ind. Med.* 49: 73–84, 1992.
5. **American Thoracic Society.** Snowbird workshop on standardization of spirometry. *Am. Rev. Respir. Dis.* 119: 831–838, 1979.
6. **Colton, T.** *Statistics in Medicine.* Boston, MA: Little, Brown, 1974.
7. **Epler, G. R., T. C. McLoud, E. A. Gaensler, J. P. Mikus, and C. B. Carrington.** Normal chest roentgenograms in chronic diffuse infiltrative lung disease. *N. Engl. J. Med.* 298: 934–939, 1978.
8. **Feagle, S. R., and D. J. Skorton.** Quantitative methods in cardiac imaging: an introduction to digital image processing. In: *Cardiac Imaging*, edited by M. L. Marcus, H. R. Schulbert, D. J. Skorton, and G. L. Wolf. Philadelphia, PA: Saunders, 1991, p. 72–86.
9. **Ferris, B. G.** Epidemiology Standardization Project (American Thoracic Society). *Am. Rev. Respir. Dis.* 118: 1–120, 1978.
10. **Gaensler, E. A., and C. B. Carrington.** Open biopsy for chronic diffuse infiltrative lung disease: clinical, roentgenographic, and physiological correlations in 502 patients. *Ann. Thorac. Surg.* 30: 411–426, 1980.
11. **Goldman, H. I., and M. R. Becklake.** Respiratory function tests: normal values at median altitudes and the prediction of normal results. *Am. Rev. Tuberc.* 79: 457–467, 1959.
12. **Gould, G. A., W. MacNee, A. McLean, P. M. Warren, A. Redpath, J. J. K. Best, D. Lamb, and D. C. Flenley.** CT measurement of lung density in life can quantitate distal airspace enlargement: an essential defining feature of human emphysema. *Am. Rev. Respir. Dis.* 137: 380–392, 1988.
13. **Haendchen, R. V., K. Ong, M. C. Fishbein, W. Zwehl, S. Meerbaum, and E. Corday.** Early differentiation of infarcted and noninfarcted reperfused myocardium in dogs by quantitative

analysis of regional myocardial echo amplitudes. *Circ. Res.* 57: 718–728, 1985.

14. **International Labour Office.** *Guidelines for the Use of the ILO International Classification of Radiographs of Pneumoconioses.* Geneva: ILO, 1980, no. 22. (Occup. Saf. Health Ser.)
15. **Kalender, W. A., H. Fichte, W. Bautz, and M. Skalej.** Semiautomatic evaluation procedures for quantitative CT of the lung. *J. Comput. Assisted Tomogr.* 15: 248–255, 1991.
16. **Kalender, W. A., R. Rienmüller, W. Seissler, J. Behr, M. Welke, and H. Fichte.** Measurement of pulmonary parenchymal attenuation: use of spirometric gating with quantitative CT. *Radiology* 175: 265–268, 1990.
17. **Katsuragawa, S., K. Doi, and H. MacMahon.** Image feature analysis and computer-aided diagnosis in digital radiography: classification of normal and abnormal lungs with interstitial disease in chest images. *Med. Phys. NY* 16: 38–44, 1989.
18. **Kinsella, M., N. L. Müller, R. T. Abboud, N. J. Morrison, and A. DyBuncio.** Quantitation of emphysema by computed tomography using a "density mask" program and correlation with pulmonary function tests. *Chest* 97: 315–321, 1990.
19. **Kipen, H. M., R. Lilis, Y. Suzuki, J. A. Valciukas, and I. J. Selikoff.** Pulmonary fibrosis in asbestos insulation workers with lung cancer: a radiological and histopathological evaluation. *Br. J. Ind. Med.* 44: 96–100, 1987.
20. **Kleinbaum, D. G., and L. L. Kupper.** *Applied Regression Analysis and Other Multivariate Methods.* Boston, MA: Duxbury, 1982.
21. **Morris, J. F., A. Koski, and L. C. Johnson.** Spirometric standards for healthy nonsmoking adults. *Am. Rev. Respir. Dis.* 103: 57–67, 1971.
22. **Müller, N. L., and R. R. Miller.** Computed tomography of chronic diffuse infiltrative lung disease. Parts 1 and 2. *Am. Rev. Respir. Dis.* 142: 1206–1215; 1440–1448, 1990.
23. **Müller, N. L., C. A. Staples, R. R. Miller, and R. T. Abboud.** "Density mask": an objective method to quantitate emphysema using computed tomography. *Chest* 94: 782–787, 1988.
24. **Müller, N. L., C. A. Staples, R. R. Miller, S. Vedal, W. M. Thurlbeck, and D. N. Ostrow.** Disease activity in idiopathic pulmonary fibrosis: CT and pathologic correlation. *Radiology* 165: 731–734, 1987.
25. **Musch, D. C., J. R. Landis, I. T. T. Higgins, J. C. Gilson, and R. N. Jones.** An application of kappa-type analysis to interobserver variation in classifying chest radiographs for pneumoconiosis. *Stat. Med.* 3: 73–83, 1984.
26. **Pietrzyk, U., K. Herholz, and W.-D. Heiss.** Three-dimensional alignment of functional and morphological tomograms. *J. Comput. Assisted Tomogr.* 14: 51–59, 1990.
27. **Reger, R. B., and W. K. C. Morgan.** On the factors influencing consistency in the radiologic diagnosis of pneumoconiosis. *Am. Rev. Respir. Med.* 102: 905–915, 1970.
28. **Robinson, P. J., and L. Kreel.** Pulmonary tissue attenuation with computed tomography: comparison of inspiration and expiration scans. *J. Comput. Assisted Tomogr.* 3: 740–748, 1979.
29. **Sartoris, D. J., D. Resnick, D. Gershuni, D. Bielecki, and M. Meyers.** Computed tomography with multiplanar reformation and 3-dimensional image analysis in the preoperative evaluation of ischemic necrosis of the femoral head. *J. Rheumatol.* 13: 153–163, 1986.
30. **Schwartz, D. A., L. J. Fuortes, J. R. Galvin, L. E. Schmidt, B. N. Leistikow, F. P. LaMarte, and J. A. Merchant.** Asbestos-induced pleural fibrosis and impaired lung function. *Am. Rev. Respir. Dis.* 141: 321–326, 1990.
31. **Schwartz, D. A., J. R. Galvin, S. J. Yagla, S. B. Speakman, J. A. Merchant, and G. W. Hunninghake.** Restrictive lung function and asbestos-induced pleural fibrosis: a quantitative approach. *J. Clin. Invest.* 91: 2685–2692, 1993.
32. **Skorton, D. J., H. E. Melton, N. G. Pandian, J. Nichols, S. Koyanagi, M. L. Marcus, S. M. Collins, and R. E. Kerber.** Detection of acute myocardial infarction in closed-chest dogs by analysis of regional two-dimensional echocardiographic gray-level distributions. *Circ. Res.* 52: 36–44, 1983.
33. **Staples, C. A., G. Gamsu, C. S. Ray, and W. R. Webb.** High resolution computed tomography and lung function in asbestos-exposed workers with normal chest radiographs. *Am. Rev. Respir. Dis.* 139: 1502–1508, 1989.
34. **Tully, R. J., R. W. Conners, C. A. Harlow, and G. S. Lodwick.** Towards computer analysis of pulmonary infiltration. *Invest. Radiol.* 13: 298–305, 1978.
35. **Van Ganse, W. F., B. G. Ferris, and J. E. Cotes.** Cigarette smoking and pulmonary diffusing capacity (transfer factor). *Am. Rev. Respir. Dis.* 105: 30–41, 1972.
36. **Wegener, O. H., P. Koeppe, and H. Oeser.** Measurement of lung density by computed tomography. *J. Comput. Assisted Tomogr.* 2: 263–273, 1978.
37. **Yerushalmy, J.** The statistical assessment of the variability in observer perception and description of roentgenographic pulmonary shadows. *Radiol. Clin. North Am.* 8: 381–392, 1969.
38. **Yerushalmy, J., L. H. Garland, J. T. Harkness, H. C. Hinshaw, E. R. Miller, S. J. Shipman, and H. B. Zwerling.** An evaluation of the role of serial chest roentgenograms in estimating the progress of disease in patients with pulmonary tuberculosis. *Am. Rev. Tuberc.* 64: 225–248, 1951.
39. **Zavala, D. C., and G. W. Hunninghake.** Lung lavage. In: *Recent Advances in Respiratory Medicine*, edited by D. C. Flenley and T. L. Petty. Edinburgh, UK: Livingston, 1983, p. 21–33.